

IMECE2005-80789

## MODAL BASED CORRECTION METHODS FOR THE PLACEMENT OF PIEZOCERAMIC MODULES

**Michael Rose**

Institute of Composite Structures and Adaptive Systems  
Lilienthalplatz 7  
38108 Braunschweig  
Niedersachsen  
Germany  
Email: michael.rose@dlr.de

### ABSTRACT

*Conventional Finite-Element programs are able to compute the vibration response of mechanical structures. Increasingly also so-called multi-field problems can be solved. For piezoelectric actuators and sensors, electrical degrees of freedom apart from the mechanical ones have to be considered too. The pure actuator effect can also be modelled using the coefficients of thermal expansion. But regarding the optimal placement of flat piezoceramic modules, which couple in the mechanical part through the  $d_{31}$ -effect, it proves to be advantageous to consider them after doing the computational complex modal analysis.*

*In this paper, this modal coupling approach is described in detail. It introduces an additional modelling error, because the effect of the stiffness and mass of the modules is not considered in the construction process of the functional space, from which modal shapes are derived. But due to the comparatively small contribution to the global mass and stiffness of such flat devices, this additional error can generally be accepted. Furthermore this error can be reduced to an arbitrarily small amount, if the number of retained eigenmodes is increased and the gain in computational speed is significant. For the calculations, self-written triangle elements with full electro-mechanical coupling have been used, being coded completely in MATLAB.*

*Finally the optimization procedure for the placement of the piezoceramic modules including their mass and stiffness is demonstrated for a test structure.*

**Keywords:** modal, piezo patch, optimization, smart materials.

### INTRODUCTION

Mechanical structures can be accurately described in a given frequency range by modal low order models. Changing the model usually requires a new modal analysis, which can be quite expensive, if the physical model is based on a Finite Element code with many degrees of freedom. Especially optimal placement algorithms for finding best positions and configurations of e.g. piezoelectric actuators suffer from this computational burden. This paper discusses the so-called *modal correction method* [1] to avoid further modal decompositions in the case of moderate system changes, if flat piezoceramic patches as actuators or sensors are applied to the originally passive elastic structure in certain surface domains. For this purpose the modal data, consisting of eigenfrequencies, eigenmodes and modal damping factors (assuming modal masses of unity) have to be adjusted by correction values, depending on the applied devices. From a practical point of view the flat piezoceramic patch is partitioned in triangular subdomains. A new triangle electro-mechanical bending element, based on Kirchhoff's plate theory, is used to calculate the modal stiffness and mass matrices for the adjustment of the modal equations. In addition piezoelectric coupling terms are determined and plugged into the modal equations, which are needed to consider the electrical network shunts of the ceramics. The details of this approach are fully described in [2] and only an outline is presented here for brevity. Especially the triangle elements are discussed there in full detail, including listings and verification procedures.

Starting point is the system of dynamic equations

$$\begin{aligned}\hat{M}\ddot{\mathbf{u}} + \hat{D}\dot{\mathbf{u}} + \hat{K}\mathbf{u} &= \hat{\mathbf{f}}, \quad \text{and} \\ \mathbf{M}\ddot{\mathbf{q}} + \mathbf{D}\dot{\mathbf{q}} + \mathbf{K}\mathbf{q} &= \mathbf{f}, \quad \mathbf{u} = \Phi\mathbf{q},\end{aligned}$$

with the diagonal matrices  $\mathbf{M} = \Phi^T \hat{\mathbf{M}} \Phi$ ,  $\mathbf{K} = \Phi^T \hat{\mathbf{K}} \Phi$ , the generalized force vector  $\mathbf{f} = \Phi^T \hat{\mathbf{f}}$  and the generalized displacement vector  $\mathbf{q}$ .  $\Phi$  contains the selected and columnwise ordered eigenmodes of the modal analysis and the diagonal terms of  $\mathbf{K}$  are the square values of the corresponding eigenfrequencies  $\omega_j = 2\pi f_j$ , if the modal masses are normed to unity, e.g. if  $\mathbf{M} = \mathbf{I}$  holds. The additional assumption of modal damping provides the diagonality of  $\mathbf{D} = \Phi^T \hat{\mathbf{D}} \Phi$ , which is generally not strictly true.

When the mechanical system is extended by piezoelectric actuators and sensors, some correction matrices  $\hat{\mathbf{M}}_p$  and  $\hat{\mathbf{K}}_p$  have to be added to the mass matrix  $\hat{\mathbf{M}}$  and the stiffness matrix  $\hat{\mathbf{K}}$ . These changes imply corrections in the eigenmodes  $\Phi$  and the eigenfrequencies. But under the assumption, that the new eigenmodes can be approximated by the old ones sufficiently well, another modal analysis can be avoided. Instead the old modal diagonal matrices  $\mathbf{M}$  and  $\mathbf{K}$  can be modified by the additive correction matrices  $\mathbf{M}_p = \Phi^T \hat{\mathbf{M}}_p \Phi$  and  $\mathbf{K}_p = \Phi^T \hat{\mathbf{K}}_p \Phi$ . These correction matrices can be computed very fast, because of the many zero entries in the matrices  $\hat{\mathbf{M}}_p$  and  $\hat{\mathbf{K}}_p$ . The precision of this approach can be controlled by the number of eigenmodes, which are used. Furthermore other displacement functions can be incorporated in  $\Phi$  as well. Though non modal columns in  $\Phi$  destroy the diagonality of  $\mathbf{M}$  and  $\mathbf{K}$ , the computational burden of diagonalizing  $\mathbf{M}$  and  $\mathbf{K}$  with modal techniques is quite low, because of the comparatively low order of  $\mathbf{M}$  and  $\mathbf{K}$ . This also holds for the corrected matrices  $\mathbf{M} + \mathbf{M}_p$  and  $\mathbf{K} + \mathbf{K}_p$ , which are non-diagonal in general too.

Suppose the modal matrices  $\mathbf{M}$ ,  $\mathbf{D}$  and  $\mathbf{K}$  are known together with the generalized modal force vector  $\mathbf{f}$ . Let  $\mathbf{p}_i$  denote the nodes of a surface mesh of the structure, where piezoceramic patches can be placed. For all nodes  $\mathbf{p}_i$ , the displacement components

$$\mathbf{u}_i = [u_i \ v_i \ w_i \ \varphi_{xi} \ \varphi_{yi} \ \varphi_{zi}]^T$$

of each eigenmode are also assumed to be known. By suitable interpolation algorithms, the displacement components of arbitrary points on the meshed surface can be obtained. Therefore the three nodal displacement vectors of an arbitrarily placed triangular element can be determined. The non-zero components of  $\hat{\mathbf{M}}_p$  and  $\hat{\mathbf{K}}_p$  are given by the two  $15 \times 15$ -element matrices of the triangle bending element, describing a part of the applied piezoceramic patch. By left and right multiplication of the corresponding displacement components  $\mathbf{u}_i$  and  $\mathbf{u}_j$  of the  $i$ -th and

$j$ -th eigenmode, the matrices  $\mathbf{M}_p$  and  $\mathbf{K}_p$  can be calculated. The  $15 \times 1$ -piezoelectric coupling vector is obtained in a similar way.

## 1 An electro-active triangular bending element

The development of triangular finite bending elements is extensively investigated in the literature. A detailed discussion of the advantages and disadvantages of different concepts is given in [3]. Roughly speaking triangular bending elements can be problematic, but the simplicity of creating triangular meshes for placement strategies, in combination with the simple algorithms for partitioning polygonal areas into triangular subdomains outweighs the disadvantages of these elements, which are mainly concerned in the correct determination of the material stresses. Indeed these are not needed for vibration analysis in the topic of adaptive systems. Generally so-called compatible elements are less efficient than incompatible elements, but the former are always convergent [3]. For this reason, we coded two active bending elements (one compatible Clough-Tocher macro element [3] and one incompatible so-called Specht element [4]) in the matrix language *MATLAB*. Both of them performed equally well in tests. Therefore only the latter faster element is used here. Note that compatibility implies monotone convergence, but requires  $C^1$ -continuity for the bending displacement  $w$  in the Kirchhoff theory. Extending this theory by membrane displacements, the kinematic variability is given by

$$\mathbf{u} = \begin{bmatrix} u - z w_{,x} \\ v - z w_{,y} \\ w \end{bmatrix}, \quad z_m - \frac{h}{2} \leq z \leq z_m + \frac{h}{2}. \quad (1)$$

The displacements  $u(x, y)$ ,  $v(x, y)$  and  $w(x, y)$  are related to the middle surface  $z = 0$ , the  $x$ - and  $y$ - cross sections are rotated by  $\Phi_x(x, y) = w_{,y}(x, y)$  and  $\Phi_y(x, y) = -w_{,x}(x, y)$ . The width of the piezoceramic patch of thickness  $h$  has a distance of  $z_m$  to the middle surface. This leads to the linearized strain terms

$$\boldsymbol{\varepsilon} = \begin{bmatrix} \varepsilon_x \\ \varepsilon_y \\ \gamma_{xy} \end{bmatrix} = \begin{bmatrix} u_{,x} - z w_{,xx} \\ v_{,y} - z w_{,yy} \\ u_{,y} + v_{,x} - 2z w_{,xy} \end{bmatrix}.$$

The plain stress assumption implies  $\sigma_z = \tau_{xz} = \tau_{yz} = 0$  and replaces the incompatible restrictions  $\varepsilon_z = \gamma_{xz} = \gamma_{yz} = 0$ , which can formally be derived from (1). The material law of the electro-mechanically coupled piezoceramic patch, reduced to the relevant stress and strain components, is given by

$$\begin{bmatrix} \varepsilon_x \\ \varepsilon_y \\ \gamma_{xy} \end{bmatrix} = \frac{1}{E} \begin{bmatrix} 1 & -\nu & 0 \\ -\nu & 1 & 0 \\ 0 & 0 & 2(1+\nu) \end{bmatrix} \begin{bmatrix} \sigma_x \\ \sigma_y \\ \tau_{xy} \end{bmatrix} + \begin{bmatrix} d_{31} \\ d_{31} \\ 0 \end{bmatrix} E_3, \quad (2)$$

with the electric field having only one non-zero component  $E_3$  in  $z$ -direction and assuming isotropic passive material properties. This can be transformed into

$$\begin{bmatrix} \sigma_x \\ \sigma_y \\ \tau_{xy} \end{bmatrix} = \underbrace{\frac{E}{1-\nu^2} \begin{bmatrix} 1 & \nu & 0 \\ \nu & 1 & 0 \\ 0 & 0 & \frac{1-\nu}{2} \end{bmatrix}}_{=C} \begin{bmatrix} \varepsilon_x \\ \varepsilon_y \\ \gamma_{xy} \end{bmatrix} - \underbrace{\begin{bmatrix} e_{31}^* \\ e_{31}^* \\ 0 \end{bmatrix}}_{=E} E_3. \quad (3)$$

The star in  $e_{31}^* = \frac{E}{1-\nu} d_{31}$  indicates, that this component is not directly related to the three dimensional tensor  $e_{ij}$ , because the plane stress assumption has been used. Sometimes the partition

$$C = \frac{E}{2(1-\nu^2)} \begin{bmatrix} 1 & 1 & 0 \\ 1 & -1 & 0 \\ 0 & 0 & 1 \end{bmatrix} \begin{bmatrix} 1+\nu & 0 & 0 \\ 0 & 1-\nu & 0 \\ 0 & 0 & 1-\nu \end{bmatrix} \begin{bmatrix} 1 & 1 & 0 \\ 1 & -1 & 0 \\ 0 & 0 & 1 \end{bmatrix}$$

is advantageous. To model piezo patches with homogenized material coefficients, which have inherent anisotropies in the  $xy$ -plane, as in the case of comb electrodes [5] for using the so-called  $d_{33}$ -effect, the more general formulas

$$C = E^* \begin{bmatrix} 1 & \nu & 0 \\ \nu & \nu_E & 0 \\ 0 & 0 & \frac{1-\nu_G \nu}{2} \end{bmatrix} \quad \text{and} \quad E = e^* \begin{bmatrix} 1 \\ \nu_e \\ 0 \end{bmatrix} = \begin{bmatrix} e_x^* \\ e_y^* \\ 0 \end{bmatrix} \quad (4)$$

have to be used for  $C$  and  $E$ . The new dimension less parameters  $\nu_E$ ,  $\nu_G$  and  $\nu_e$  are equal to one in the special case of passive isotropy.  $C$  and  $E$  from (4) are shown for a fibre angle of  $\varphi = 0$ , but they can easily be transformed to other fibre angles by using the tensor laws.

Neglecting the rotational inertia terms, the mass matrix  $M_p$  and the stiffness matrix  $K_p$ , as well as the electro-mechanical coupling vector  $f_p$  of the ceramic patch can be obtained from the variational formulation

$$\delta q^T \left( M_p \ddot{q} + K_p q - \underbrace{f_p}_{=U} h E_3 \right) = \int_V \left( \rho \begin{bmatrix} \delta u \\ \delta v \\ \delta w \end{bmatrix}^T \begin{bmatrix} \ddot{u} \\ \ddot{v} \\ \ddot{w} \end{bmatrix} + \begin{bmatrix} \delta \varepsilon_x \\ \delta \varepsilon_y \\ \delta \gamma_{xy} \end{bmatrix}^T \begin{bmatrix} \sigma_x \\ \sigma_y \\ \tau_{xy} \end{bmatrix} \right) dV. \quad (5)$$

Using the Gauß integral theorem,  $f_p$  possesses the alternative

representation

$$\begin{aligned} \delta q^T f_p &= \frac{e_{31}^*}{h} \int_V (\delta \varepsilon_x + \delta \varepsilon_y) dV \\ &= \frac{e_{31}^*}{h} \int_{z_m-h/2}^{z_m+h/2} \int_{\partial A} \begin{bmatrix} \delta u - z \delta w_{,x} \\ \delta v - z \delta w_{,y} \end{bmatrix}^T \mathbf{n} ds dz \\ &= e_{31}^* \int_{\partial A} \left( \begin{bmatrix} \delta u \\ \delta v \end{bmatrix}^T \mathbf{n} - z_m \frac{\partial \delta w}{\partial \mathbf{n}} \right) ds, \end{aligned} \quad (6)$$

with the normalized outer normal vector  $\mathbf{n}$  of the base area  $A$  of the piezoceramic patch. Using the anisotropic material law (4), the variational formulation is given by

$$\begin{aligned} \delta q^T f_p &= \frac{1}{h} \int_V (e_x^* \delta \varepsilon_x + e_y^* \delta \varepsilon_y) dV \\ &= \int_{\partial A} \begin{bmatrix} e_x^* n_x \\ e_y^* n_y \end{bmatrix}^T \left( \begin{bmatrix} \delta u \\ \delta v \end{bmatrix} - z_m \begin{bmatrix} \delta w_{,x} \\ \delta w_{,y} \end{bmatrix} \right) ds. \end{aligned}$$

Anisotropic material laws are not considered in the *MATLAB*-implementation, because the classic  $d_{31}$ -patches have been of main interest to our department so far [6]. The implementation can easily be extended to the anisotropic case though. Attention must be given to the correct treatment of the fibre angle in the mesh generation, but this is a problem of careful book keeping. In addition to the modified material stiffness  $C$  of (4), the representation of the coupling vectors  $f_p$  has to be adapted as shown.

## 2 Low order modal electro-mechanical systems

To complete the discussion about the modal electro-mechanical system equations, the sensoric properties of the piezo devices have to be considered. In addition to the actuatoric equation (5) in variational form, the corresponding sensoric equations, in combination with the equations of the electric network are needed. This requires the full set of constitutive material properties, which extend (3) by

$$D_3 = \begin{bmatrix} d_{31} \\ d_{31} \\ 0 \end{bmatrix}^T \begin{bmatrix} \sigma_x \\ \sigma_y \\ \tau_{xy} \end{bmatrix} + \epsilon_{33}^\sigma E_3 = \begin{bmatrix} e_{31}^* \\ e_{31}^* \\ 0 \end{bmatrix}^T \begin{bmatrix} \varepsilon_x \\ \varepsilon_y \\ \gamma_{xy} \end{bmatrix} + \epsilon_{33}^* E_3$$

with  $\epsilon_{33}^* = \epsilon_{33}^\sigma - \frac{2E}{1-\nu} d_{31}^2$ .

$\epsilon_{33}^\sigma$  denotes the dielectric constant of the piezoceramic material in  $z$ -direction, related to constant mechanical stress  $\sigma$ . Again the star in  $\epsilon_{33}^*$  reminds on the assumed plane stress distribution. The mechanical coupling term with the same piezoelectric material

coefficient  $d_{31}$  as in equation (2) results on energetic considerations, which are also responsible for the symmetry of the material stiffness matrix  $C$ . There are no dissipating terms in this physical model and the piezoceramic modul is an ideal energy transformer. The energy loss in practical applications leads to non-constant hysteretic material coefficients, which are not considered in the linear theory, upon which this derivation is based.

### 3 The generalized electro-mechanical coupling coefficient

If the electrical field  $E_3$  as state variable is independent from the mechanical displacement field, the variation of the electrical quantities can be done independent from the mechanical variation. This implies

$$\int_V \delta E_3 D_3 dV - \int_{\partial V} \delta \varphi \hat{q} dA = \int_V \delta E_3 D_3 dV + \int_{\partial V} \delta E_3 z \hat{q} dA = 0$$

with the variation of the electric potential  $\delta \varphi = -z \delta E_3$  and the prescribed surface charge density  $\hat{q}$ . It should be mentioned, that here as well as in the material law used above the idealization  $E_1 = E_2 = 0$  was made. The charge of the upper electrode of the patch is given by  $\hat{Q} = A \hat{q}$ , the lower charge therefore by  $-\hat{Q}$ . The constance of  $E_3$  and  $\delta E_3$  induces

$$\delta E_3 e_{31}^* \int_V (\varepsilon_x + \varepsilon_y) dV + h^2 \delta E_3 C_p E_3 + h \delta E_3 \hat{Q} = 0,$$

with the capacity  $C_p = \varepsilon_{33}^* A/h$  of the completely clamped ceramic. The coupling coefficients  $d_{ij}$  are based on a polarization in positive  $z$ -direction. But the polarization field is usually established by a positive electrical voltage at the upper electrode. This can be respected by changing the signs of the coupling coefficients  $d_{ij}$  or  $e_{ij}$  respectively. The same effect can be achieved by changing the sign of the electric voltage  $U$  and the electric charge  $Q$  in the equations. This implies  $U = h E_3$ ,  $Q = -\hat{Q}$  and

$$\frac{e_{31}^*}{h} \int_V (\varepsilon_x + \varepsilon_y) dV + C_p U = Q.$$

In comparison with equation (6) it follows, that the integral can also be written as  $\mathbf{q}^T \mathbf{f}_p$ , which also holds in case of an anisotropic material law. With (5) a compact form of the pure actuator and sensor equations is given by

$$\mathbf{M}_p \ddot{\mathbf{q}}_m + \mathbf{D}_p \dot{\mathbf{q}}_m + \mathbf{K}_p \mathbf{q}_m - \mathbf{f}_p U = \mathbf{f}_m, \quad (7)$$

$$\mathbf{f}_p^T \mathbf{q}_m + C_p U = Q, \quad (8)$$

with the mechanical state variables  $\mathbf{q}_m = \mathbf{q}$ . Equation (5) has been extended by the viscous damping term  $\mathbf{D}_p \dot{\mathbf{q}}_m$  and the force vector  $\mathbf{f}_m$  of an outer patch excitation. In the case of several ceramic modules, whose electrodes are not connected galvanically, the actuator equation has to be modified by coupling terms of the form  $-\mathbf{f}_{p_k} U_k$  for the  $k$ -th patch, and for each patch a corresponding sensor equation can be buildt. The complete system needs additional differential equations, involving the electric currents  $\dot{Q}_k$  and voltages  $U_k$  to describe the electrical network. Two special cases are given by galvanically shunted ceramics ( $U \equiv 0$ ) and on the other hand by ceramic patches with open electrodes ( $Q \equiv 0$ ):

$$U \equiv 0: \quad \mathbf{M}_p \ddot{\mathbf{q}}_m + \mathbf{D}_p \dot{\mathbf{q}}_m + \mathbf{K}_p^E \mathbf{q}_m = \mathbf{f}_m,$$

$$Q^E = \mathbf{f}_p^T \mathbf{q}_m, \quad \mathbf{K}_p^E = \mathbf{K}_p.$$

$$Q \equiv 0: \quad \mathbf{M}_p \ddot{\mathbf{q}}_m + \mathbf{D}_p \dot{\mathbf{q}}_m + \mathbf{K}_p^D \mathbf{q}_m = \mathbf{f}_m,$$

$$U^D = -\frac{1}{C_p} \mathbf{f}_p^T \mathbf{q}_m, \quad \mathbf{K}_p^D = \mathbf{K}_p + \mathbf{f}_p C_p^{-1} \mathbf{f}_p^T.$$

Open ceramics therefore have a higher effective mechanical stiffness and higher eigenfrequencies than shunted ceramics. One measure of the authority, a piezo patch possesses on the  $j$ -th eigenmode, is given by the dimensionless so-called *generalized electro-mechanical coupling coefficient* (first mentioned in [7] and later used by several authors, e.g. [8, 9, 10])

$$\begin{aligned} \kappa_j^2 &= \frac{\omega_j^{D^2} - \omega_j^{E^2}}{\omega_j^{E^2}} \approx \frac{1}{C_p} \frac{(\boldsymbol{\psi}_j^T \mathbf{f}_p)^2}{\boldsymbol{\psi}_j^T (\mathbf{K} + \mathbf{K}_p) \boldsymbol{\psi}_j} \\ &\approx \frac{1}{C_p} \frac{(\boldsymbol{\psi}_j^T \mathbf{f}_p)^2}{\boldsymbol{\psi}_j^T \mathbf{K} \boldsymbol{\psi}_j}. \end{aligned} \quad (9)$$

$\omega_j^E$  and  $\omega_j^D$  are the eigenfrequencies of the system with shunted and open electrodes respectively. The first approximation holds under the assumption, that the switching from shunted to open electrodes only slightly changes the  $j$ -th eigenvector  $\boldsymbol{\psi}_j$  of the eigenproblem  $(\mathbf{K} + \mathbf{K}_p) \boldsymbol{\psi} = \omega^2 (\mathbf{M} + \mathbf{M}_p) \boldsymbol{\psi}$ . The second approximation assumes a negligible modal stiffness of the piezo patch with respect to the modal stiffness of the passive system. In this case and for constant patch area (and therefore constant capacity  $C_p$ ),  $\kappa_j$  is proportional to the modal coupling  $|\boldsymbol{\psi}_j^T \mathbf{f}_p|$ . If  $\mathbf{K}$  and  $\mathbf{M}$  or  $\mathbf{K} + \mathbf{K}_p$  and  $\mathbf{M} + \mathbf{M}_p$  are diagonal matrices of the modal masses of unity and of the squares  $\omega_j^2$ , the last approximation together with  $e_j = \boldsymbol{\psi}_j$  gives the simple relation

$$\kappa_j^2 \approx \frac{(e_j^T \mathbf{f}_p)^2}{C_p \omega_j^2}. \quad (10)$$

For isolated eigenfrequencies, the other eigenmodes can be neglected in the frequency neighborhood of  $\omega_j$  and introducing the scalar quantities

$$\begin{Bmatrix} m \\ d \\ k \end{Bmatrix} = \psi_j^T \begin{Bmatrix} M + M_p \\ D + D_p \\ K + K_p \end{Bmatrix} \psi_j, \quad (11)$$

$$f = \psi_j^T \mathbf{f}_m, \quad a = \psi_j^T \mathbf{f}_p, \quad \mathbf{q}_m \approx q \psi_j, \quad (12)$$

the electro-mechanical system approximatively is described by

$$\begin{aligned} m \ddot{q} + d \dot{q} + k q - a U &= f, \\ a q + C_p U &= Q. \end{aligned}$$

With  $k = \omega^2 m$ ,  $d = 2\xi\omega m$  and  $\dot{Q} = I$ , the eigenfrequency  $\omega$ , the Lehr damping measure  $\xi$  and the electric current are substituted into the equations. An application of the Laplace transformation with the frequency variable  $s$  leads to

$$\Phi(s) := \frac{q}{q_{\text{statisch}}} = \frac{q}{f/k} = \frac{\omega^2}{s^2 + 2\xi\omega s + \omega^2 \left(1 - \frac{a U}{k q}\right)},$$

$$I = s a q + s C_p U.$$

Let  $Z$  denote the impedance of an electric network, connected to the electrodes of the piezo patch under consideration. This implies  $U = -ZI$ , because  $I$  is the current, flowing into the piezo capacitor. The impedance of the capacity of the piezo patch is given by  $Z^D = 1/s C_p$ . Denoting the impedance of a parallel circuit by

$$Z || Z^D = \frac{1}{\frac{1}{Z} + \frac{1}{Z^D}}$$

gives for the frequency function from the displacement  $q$  to the electrical voltage  $U$  the relation

$$\frac{U}{q} = -\frac{a}{C_p} \frac{Z || Z^D}{Z^D}.$$

Because of  $\kappa^2 = a^2/k C_p$ ,

$$\Phi(s) = \frac{1}{\bar{s}^2 + 2\xi\bar{s} + 1 + \kappa^2 \bar{Z}}, \quad s = \omega \bar{s}, \quad \bar{Z} = \frac{Z || Z^D}{Z^D} \quad (13)$$

holds, introducing the normalized Laplace variable  $\bar{s}$  with respect to the frequency  $\omega$ . This expression underlines the significance

of the generalized coupling coefficient  $\kappa$  for the integration of electrical networks via their impedance into modal system descriptions. Following the abbreviations from [7] by introducing the electrical damping rate  $r = \omega C_p R$ , the electrical resonance frequency  $\omega_e = 1/\sqrt{L C_p}$  and the dimensionless tuning fraction  $\delta = \omega_e/\omega$ , the dimensionless impedances of a single resistor  $R$  or a seriell  $RL$ -circuit are obtained by

$$\bar{Z}_R = \frac{r\bar{s}}{1 + r\bar{s}}, \quad \bar{Z}_{RL} = \frac{\delta^2 r\bar{s} + \bar{s}^2}{\delta^2 + \delta^2 r\bar{s} + \bar{s}^2}.$$

Galvanically shunted ceramics have the impedance  $\bar{Z} = \bar{Z}^E = 0$  and ceramics with open electrodes the impedance  $\bar{Z} = \bar{Z}^D = 1$ , which together with (13) again implies the defining equation (9) for  $\kappa$ . Hagood and Flotow suggest in [7] in case of low structural damping  $\xi$  for the serial  $RL$ -network the values

$$\delta_{\text{TF}}^{\text{opt}} = \sqrt{1 + \kappa^2}, \quad r_{\text{TF}}^{\text{opt}} = \frac{\sqrt{2}\kappa}{1 + \kappa^2}, \quad \max_{\omega} |\Phi_{\text{TF}}^{\text{opt}}(i\omega)| \approx \frac{\sqrt{2}}{\kappa\sqrt{1 + \kappa^2}} \quad (14)$$

to obtain approximately optimal damping for  $\Phi(s)$  in the neighborhood of the eigenfrequency  $\omega$ . With (14) and the definition of the dimensionless coefficients, the electrical quantities  $R$  and  $L$  can directly be calculated. Furthermore the approximative maximum of  $|\Phi_{\text{TF}}^{\text{opt}}(i\omega)|$  can be used as objective function in optimal placement algorithms. Equation (14) reveals a direct correspondance of the effective damping of a serial  $RL$ -circuit to the generalized piezoelectric coupling coefficient  $\kappa$ .

The optimal reduction in decibel of the maximum amplitude of  $\Phi(s)$  for serial  $RL$ -circuits is displayed in figure 1 for different coupling coefficients  $\kappa^2 \in [0, 1/10]$  and Lehr damping ratios  $\xi$ . Other intervals for  $\kappa$  have approximately the same curves: For  $\kappa_j^2 \in [0, 1/10^j]$ , the values  $\kappa_1^2 = 10\kappa_2^2 = 100\kappa_3^2$  correspond to the damping ratios  $\xi_1 \approx 3.22\xi_2 \approx 10.3\xi_3$ . The curves from figure 1 have been obtained by numerical optimization procedures. The theory of one mass oscillators and the approximation (14) yield

$$\max_{\omega} |\Phi_{\kappa=0}(i\omega)| = \frac{1/2\xi}{\sqrt{1 - \xi^2}}, \quad \max_{\omega} |\Phi_{\xi=0}(i\omega)| \approx \frac{\sqrt{2}/\kappa}{\sqrt{1 + \kappa^2}}.$$

By empirical combination of this border cases, it has been verified numerically, that the rule of thumb

$$\frac{\max_{\omega} |\Phi_{\kappa=0}(i\omega)|}{\max_{\omega} |\Phi(i\omega)|} \approx 1 + \sqrt{\frac{\kappa^2(1 + \kappa^2)}{8\xi^2(1 - \xi^2)}}, \quad \xi < 1\%$$

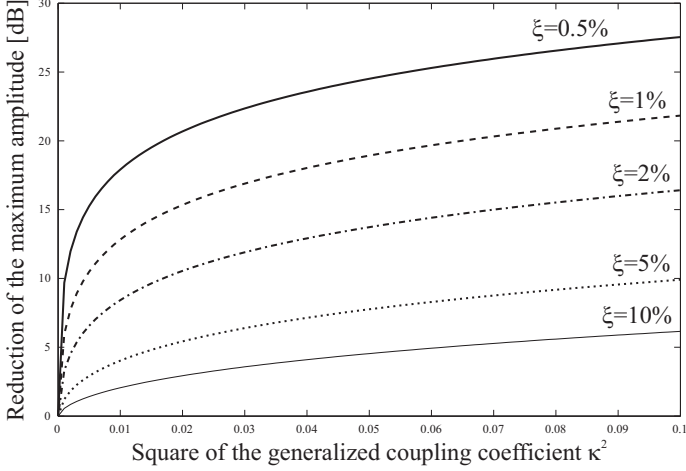


Figure 1. OPTIMAL REDUCTION in [dB] of  $\max |\Phi(i\omega)|$ .

supplies an acceptable approximation of the curves from figure 1 in decibel. The equations (7,8) can be considered for several columns of  $\Psi$  simultaneously, if the modal masses are equal to unity. By introducing the matrix quantities

$$\begin{aligned} \mathbf{I} &= \Psi^T (\mathbf{M} + \mathbf{M}_p) \Psi, & \mathbf{f} &= \Psi^T \mathbf{f}_m, \\ 2\Xi \Delta &= \Psi^T (\mathbf{D} + \mathbf{D}_p) \Psi, & \mathbf{a} &= \Psi^T \mathbf{f}_p, \\ \Delta^2 &= \Psi^T (\mathbf{K} + \mathbf{K}_p) \Psi, & \mathbf{q}_m &\approx \Psi \mathbf{q}, \end{aligned}$$

the equations of a multifrequent electro-mechanical model

$$\begin{aligned} \ddot{\mathbf{q}} + 2\Xi \Delta \dot{\mathbf{q}} + \Delta^2 \mathbf{q} - \mathbf{a} U &= \mathbf{f}, \\ \mathbf{a}^T \mathbf{q} + C_p U &= Q \end{aligned}$$

can be derived similar to equations (11,12). Again several patches can be incorporated by summation of the coupling forces  $-\mathbf{a}_k U_k$  in the actuator matrix equation and using multiple sensor equations for the quantities  $\mathbf{q}$ ,  $U_k$  and  $Q_k$ .  $\Delta$  is a diagonal matrix, containing the eigenfrequencies of the system for short circuited ceramic electrodes and the diagonal matrix  $\Xi$  contains the corresponding Lehr damping ratios. As mentioned before, the assumption has been made, that the transformed damping matrix  $\Psi^T (\mathbf{D} + \mathbf{D}_p) \Psi$  is close enough to a diagonal matrix. Transforming this equations in the Laplace domain and substituting the normalized impedance  $\bar{Z}$  from equation (13) of shunted electrical networks, the system of equations

$$\begin{aligned} (s^2 \mathbf{I} + 2s\Xi \Delta + \Delta^2 (\mathbf{I} + \bar{Z} \mathbf{A}_\kappa)) \mathbf{q} &= \mathbf{f}, \\ U &= -\frac{\bar{Z}}{C_p} \mathbf{a}^T \mathbf{q}, \quad \mathbf{A}_\kappa = \frac{1}{C_p} \Delta^{-2} \mathbf{a} \mathbf{a}^T \end{aligned}$$

results, which is quite similar to the scalar case. The transfer function from  $\mathbf{f}(s)$  to  $\mathbf{q}(s)$  can be determined and optimizations are possible by using appropriate norms.

The special case of multiple eigenfrequencies, which can be used as approximation for a cluster of closely related eigenfrequencies, occurs, if certain symmetries exist, e.g. the rotational symmetry of a circular plate. If the electro-mechanical system is reduced to the frequency range close to the multiple eigenfrequency  $\omega$ , neglecting other eigenmodes from distinct eigenfrequencies, with  $\Delta = \omega \mathbf{I}$  (and with  $\Xi = \xi \mathbf{I}$  for simplicity reasons) the frequency equations can be simplified to

$$((\bar{s}^2 + 2\xi \bar{s} + 1) \mathbf{I} + \bar{Z} \mathbf{A}_\kappa) \mathbf{q} = \frac{1}{\omega^2} \mathbf{f}, \quad \mathbf{A}_\kappa = \frac{1}{\omega^2 C_p} \mathbf{a} \mathbf{a}^T,$$

where the normalized frequency variable  $s = \omega \bar{s}$  was used again. The structure of this equation doesn't change, if orthogonal transformations  $\hat{\mathbf{q}} = \mathbf{Q} \mathbf{q}$ ,  $\hat{\mathbf{f}} = \mathbf{Q} \mathbf{f}$  and  $\hat{\mathbf{a}} = \mathbf{Q} \mathbf{a}$  with an arbitrary orthogonal matrix  $\mathbf{Q}$  are applied. Without loss of generality, the equation can be considered with the special coupling  $\mathbf{a} = a \mathbf{e}_1$ , which implies  $\mathbf{A}_\kappa = \kappa^2 \mathbf{e}_1 \mathbf{e}_1^T$ .  $a$  corresponds to  $\|\mathbf{a}\|$  of the untransformed system of equations.  $\bar{Z}$  influences the generalized displacement  $q_1$  as in the scalar case through the generalized electro-mechanical coupling coefficient  $\kappa$ . But the components  $q_j$  with  $j \geq 2$  are not influenced at all. This indicates, that multiple eigenfrequencies of order  $m$  can only be controlled by  $m$  galvanically separated electrical networks and a corresponding amount of piezo patches. Roughly speaking, due to the  $m$ -dimensionality of the involved eigenspace, vibrations can always *rotate* to an orientation orthogonal to the coupling vectors, if there are less than  $m$  electrical networks for the vibration reduction of the eigenmode under consideration.

#### 4 A central clamped circular plate as example

To demonstrate the modal correction method, a circular plate of thickness  $h = 3$  mm and outer radius  $r_1 = 15$  cm, which was clamped at the inner radius  $r_0 = 1$  cm is discussed now as demonstration example. Though the new triangular bending elements, which are coded in the *MATLAB* scripting language, are mainly developed to realize the modal correction of passive structures with respect to active patch devices, and the passive structural model will normally be supplied by Finite Element software packages like *ANSYS*, this demonstration example was completely modeled within *MATLAB*, using the stiffness and mass matrices from the new Specht element. Figure 2 shows the triangular mesh of 1860 nodes and 3600 elements, which was used for the discretization. It turns out, that the triangular elements assembled the corresponding matrices quite efficiently and the eigenfrequencies from a subsequent modal analysis are close to their counterparts, obtained by a comparative Finite Element calculation, which was done completely in *ANSYS*. Table 1

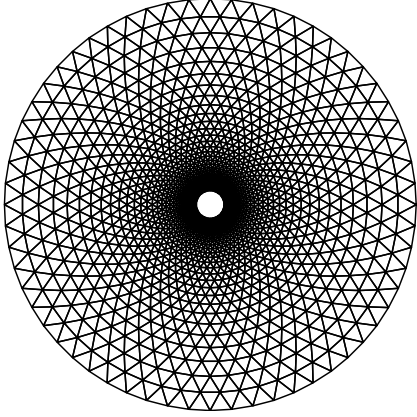


Figure 2. TRIANGULAR MESH FOR THE CIRCULAR PLATE.

$h_s$	3 mm	$h_p$	0.2 mm
$\nu_s$	0.3	$\nu_p$	0.34
$E_s$	$2.1 \cdot 10^{11} \text{N/m}^2$	$E_p$	$5.94 \cdot 10^{10} \text{N/m}^2$
$\rho_s$	$7600 \text{kg/m}^3$	$\rho_p$	$7760 \text{kg/m}^3$
$e_{31}$	$-19.2 \text{N/Vm}$	$\epsilon_{33}^S$	$1178 \cdot 8.854 \cdot 10^{-12} \text{As/Vm}$

Table 1. MATERIAL DATA FOR THE CIRCULAR PLATE.

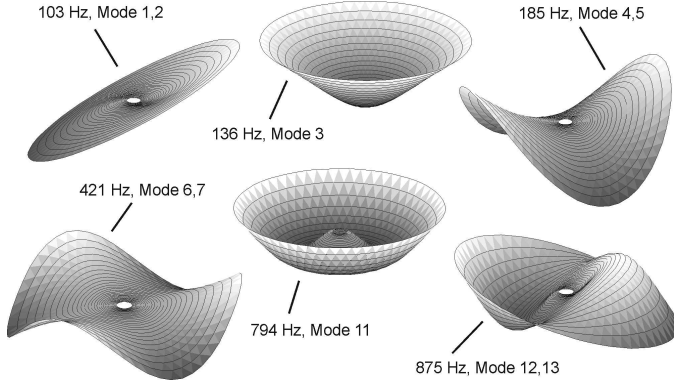


Figure 3. THE FIRST EIGENMODES OF THE CIRCULAR PLATE.

lists the material data, which was used for the plate (index  $s$ ) and for the piezo patches (index  $p$ ). The modal analysis in *MATLAB* has been done with a self-written function, based on subspace iteration, because for some strange reason, the built in *MATLAB*-function `eigs` had convergence problems. The first eigenmodes are displayed in figure 3. The rotational symmetric flat membrane mode 8 and the bending modes 9 and 10 are omitted to save space. Each eigenmode, which is not rotational symmetric, possesses the multiplicity two and can occur arbitrarily rotated around the  $z$ -axis, because of the rotational plate

symmetry. Mode 3 und mode 11 in contrast are rotational symmetric simple eigenmodes. If piezo patches are placed in equal pairs above and below the plate, membrane and bending eigenmodes can be targeted separately by equal and opposite poling of their electrodes respectively. As already discussed, there are at least two separated patches necessary to control the eigenmodes with multiplicity two. Consider now two orthogonal eigenmodes with the same eigenfrequency  $\omega_j$ . They have the same shape, the same maximum amplitude due to the fact that the modal masses are equal to unity and are rotated by some angle  $\beta_j$ . The optimal shape for the second patch can therefore be obtained from the optimal first patch by rotation with  $\beta_j$ . This implies, that for each eigenfrequency only one optimal piezo patch has to be determined, which is used twice and rotated by  $\beta_j$  in case of eigenfrequencies of multiplicity two. Of course overlapping piezo patches need additional heuristic considerations, if multiple layers are not feasible.

Each pair of piezo patches is defined by a triangle mesh, whose nodes are controlled by the underlying optimization procedure. The modal parameters (stiffness, mass, coupling vector and capacity) are calculated elementwise by the developed triangle bending element and the modal displacements at the nodes are interpolated from the known eigenmode displacements of the circular plate mesh using the *MATLAB*-function `griddata` or similar functions. The generalized piezoelectric coupling coefficient is calculated by equation (10) with or without negotiation of the changes due to the piezo mass and stiffness.

Simple patch geometries can be controlled by special parameters. If the shape of the patches is restricted to be a circular section, the four parameters  $\varphi_{p0}$ ,  $\varphi_{p1}$ ,  $r_{p0}$  and  $r_{p1}$  can be used to build the needed triangular mesh for the patch. Figure 4 shows the distribution of  $\kappa_1^2 + \kappa_2^2$  for the first pair of eigenmodes 1 and 2. Due to the fact, that the combined value  $\kappa_1^2 + \kappa_2^2$  is not changed by patch rotation around the  $z$ -axis, the start angle  $\phi_{p0} = 0$  was fixed. To visualize the result, the inner radius  $r_{p0} = 0.15\text{m}$  was fixed too. Therefore the only free parameters in this parameter study are the outer radius  $r_{p1}$  and the sector angle  $\varphi_{p1}$ .

In the case of  $r_1 = 0.15\text{m}$  and  $\phi_1 = 180^\circ$ , the combined coupling coefficient  $\kappa_1^2 + \kappa_2^2 = 0.77\%$  is far away from its optimum value  $1.93\%$ , though the strain sum  $\varepsilon_x + \varepsilon_y$  of the first two eigenmodes, which is directly related to  $\mathbf{f}_p$ , is positive in one half of the circular plate and negative in the other half. A close look to the formula for  $\kappa^2$  reveals, that a higher patch area implies a higher patch capacity, which reduces the effect, a passive electrical network can have to the mechanical structure. For active systems [11, 12, 13, 14] with unlimited energy reserves, the electric potential in the ceramic can be provided independently from its capacity. In this case the coupling term  $a$  should be maximized. But if energy is also of concern, or passive networks are used,  $\kappa$  is the better choice for the objective function of an

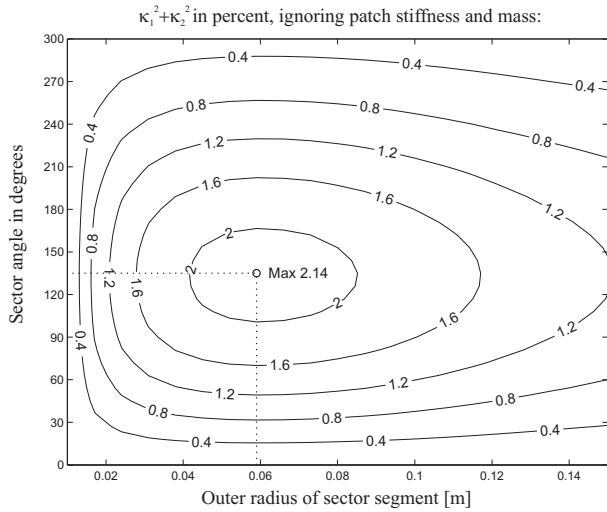
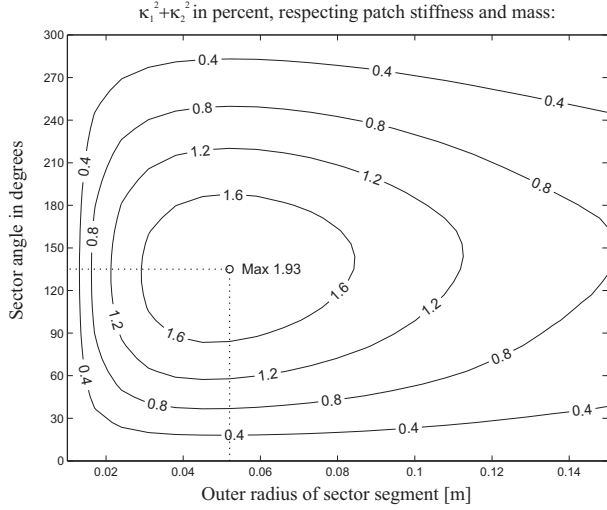


Figure 4. EFFECTIVITY OF PATCH SECTORS FOR  $j = 1, 2$ .

optimization procedure. With

$$a_j = e_{31}^* \int_A (\text{div} \begin{bmatrix} u_j \\ v_j \end{bmatrix} - z_m \Delta w_j) dA, \quad C_p = \frac{\epsilon_{33}^*}{h} A$$

the optimal placement with respect to the  $j$ -th eigenmode can be done as follows. For passive electrical networks or limited energy resources, maximize

$$\kappa_j^2 = \frac{h e_{31}^{*2}}{\omega_j^2 \epsilon_{33}^*} \cdot \left( \frac{1}{\sqrt{A}} \int_A (\text{div} \begin{bmatrix} u_j \\ v_j \end{bmatrix} - z_m \Delta w_j) dA \right)^2.$$

For active control with sufficiently high power capabilities (the higher the frequency, the more severe is this restriction), maxi-

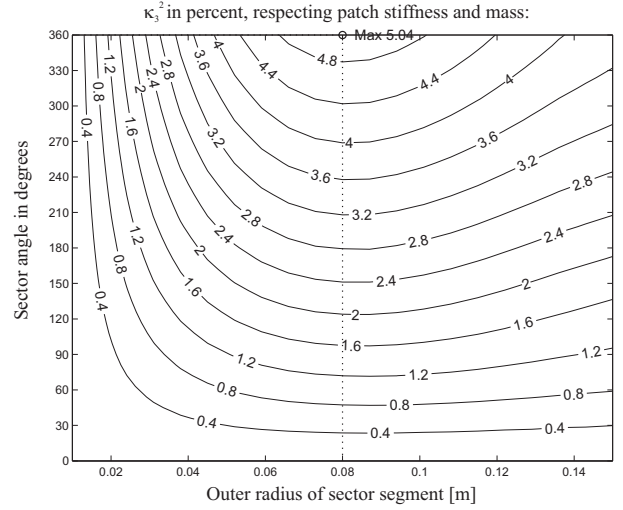


Figure 5. EFFECTIVITY OF PATCH SECTORS FOR  $j = 3$ .

mize

$$|a_j| = |e_{31}^*| \cdot \left| \int_A (\text{div} \begin{bmatrix} u_j \\ v_j \end{bmatrix} - z_m \Delta w_j) dA \right|.$$

$u_j$ ,  $v_j$  and  $w_j$  denote in this context the displacement components of the  $j$ -th eigenmode.

Figure 5 shows the distribution of the coupling coefficient for the third eigenmode. In case of the third mode, the optimum patch area for passive electrical networks covers only the inner plate with outer patch radius 0.08m, in contrast to the optimal area for active control, which covers the complete circular plate. The fourth and fifth eigenmode reveals several local maxima and the global optimum of  $\kappa_4^2 + \kappa_5^2 = 0,23\%$  is given by  $r_{p0} = 0,088$  m,  $r_{p1} = 0,15$  m,  $\phi_{p1} = 65^\circ$ . This result cannot be achieved by the previous parameter study, because of the artificial restriction  $r_{p0} = 0,01$ m, leading to the suboptimal value  $\kappa_4^2 + \kappa_5^2 = 0,065\%$ . These eigenmodes are better controlled by patches at the outer border of the plate. For even higher eigenmodes, there exist optimal shapes, lying completely in the circular plate. Figure 6 displays the strain distribution  $\epsilon_x + \epsilon_y$  and the optimal patch sector, obtained by gradient based optimization procedures for the first eigenmodes. Table 2 summarizes the calculated parameters numerically. The influence of the patch stiffness and mass to the distribution of  $\kappa$  can clearly be observed in figure 4, but the qualitative information is not changed significantly. Therefore a two step approach in the optimization of the patches seems to be promising. The comparatively costly calculation of the patch masses and stiffnesses is not done in the actual optimization of the patch shape. After convergence to the optimal shape, the mass and stiffness of the mechanical structure is updated with respect to the optimized patch configuration. These two steps are repeated until global

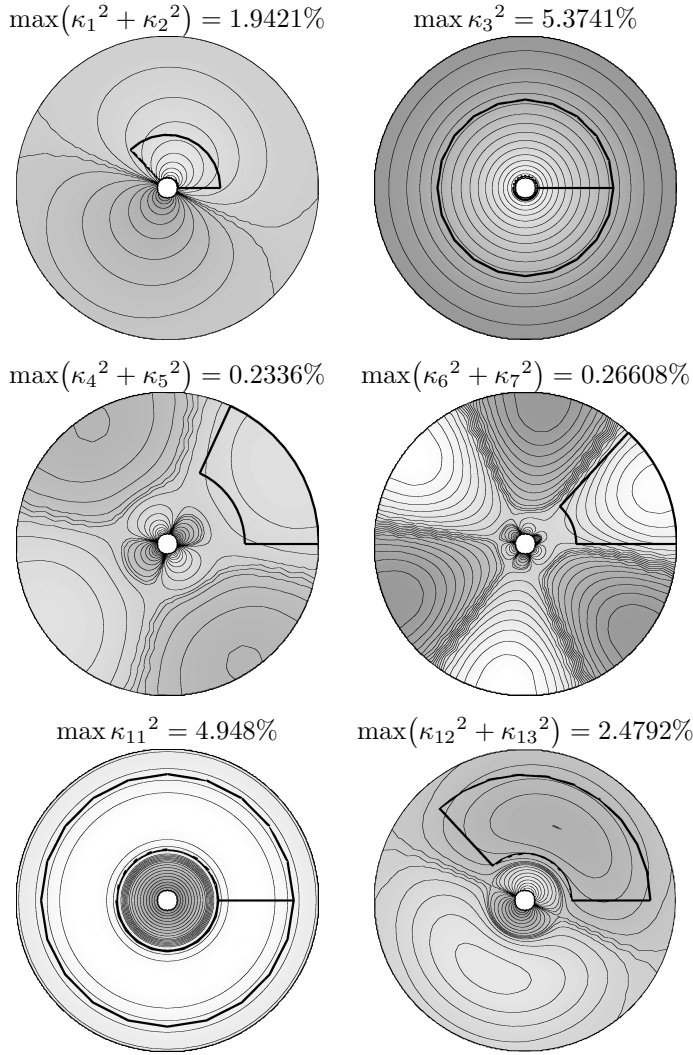


Figure 6. STRAIN DISTRIBUTION AND OPTIMAL PATCH SECTOR.

convergence is achieved. There are some drawbacks in applying this procedure to multiple eigenfrequencies, but current research is done on that topic.

Optimization of the full patch shape without considering its stiffness and mass is more simple and can be done with fast algorithms, which are currently under development. Figure 7 shows some results from these algorithms for the investigated circular plate. The displayed coupling coefficients are not directly comparable with the ones from figure 6. They are higher due to the ignored patch stiffness and mass. It is very difficult to find efficient optimization techniques, which avoid the overlapping of piezo patches for distinct eigenmodes. Therefore some heuristic compromises have to be made after optimizing the patch shapes. Figure 8 indicates a possible compromise for the first five eigenmodes of the circular plate example.

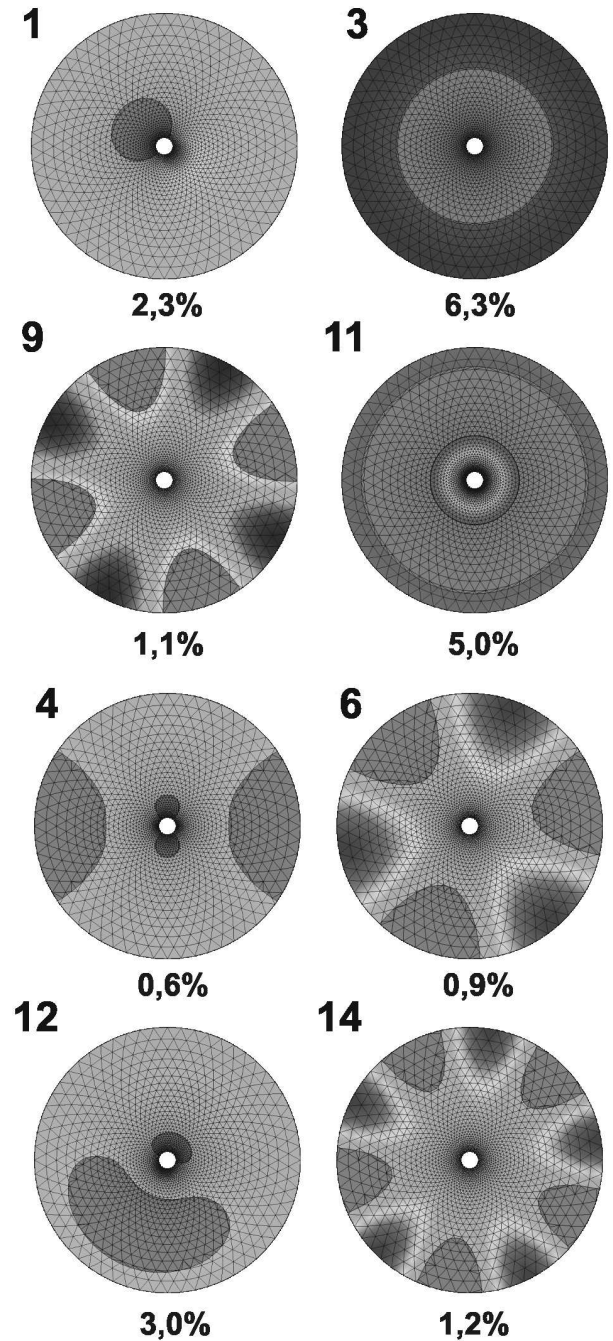


Figure 7. OPTIMAL FREE FORM PATCHES AND  $\kappa_j^2$  VALUES.

## SUMMARY

The modal correction method was discussed and especially adapted to the case of applying flat piezoelectric devices to the surface of a mechanical structure. Two active triangular bending elements were used to calculate the modal correction param-

$j$	freq.	$\beta_j$	$\sum \kappa_j^2$	$r_{p0} - r_{p1}$	$\phi_{p0} - \phi_{p1}$
1,2	106 Hz	90°	1,94%	10-55 mm	0 – 136°
3	144 Hz	-	5,37%	10-87 mm	0 – 360°
4,5	184 Hz	45°	0,23%	79-150 mm	0 – 67°
6,7	421 Hz	30°	0,27%	50-150 mm	0 – 47°
11	798 Hz	-	4,95%	51-125 mm	0 – 360°
12,13	877 Hz	90°	2,48%	47-125 mm	0 – 133°

Table 2. OPTIMAL PATCH SECTORS.

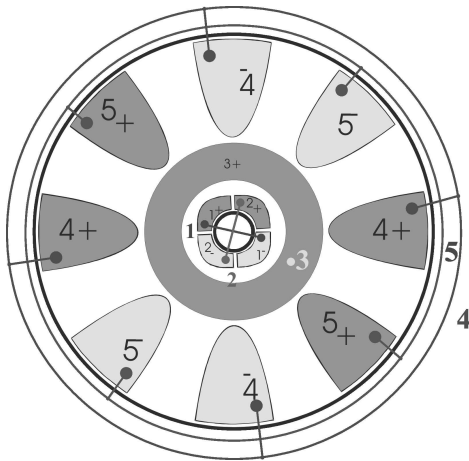


Figure 8. HEURISTIC CHOICE OF NON OVERLAPPING PATCHES.

ters for piezo patch actuators and sensors. The implementation in *MATLAB* can be found in [2]. Some objective functions have been discussed to optimize the shape of applied patches and the generalized piezoelectric coupling coefficient  $\kappa$  has been proved to be a very good choice. After presenting the complete modal equations with embedded shunt impedances, the example of the circular plate has been discussed to demonstrate the whole procedure.

## ACKNOWLEDGMENT

Thanks go to Alberto Belloli, Lucio Flavio Campanile and Stefan Homann, who contributed to this paper with several inspiring discussions.

## REFERENCES

- [1] Breitbach, E., and Niedbal, N., 1974, "Berücksichtigung von Modifikationen der in Standschwingungsversuchen untersuchten Außenlastkonfigurationen des Alpha-Jets mittels modaler Korrekturen auf der Basis der Versuchsergebnisse", DFVLR/IB-253/74/C/18, DLR Göttingen, p. 54.
- [2] Rose, M., 2004, "Modale Korrekturmethode für die Platzierung von Piezokeramischen Modulen", IB, 131-2004/43, DLR Braunschweig, p. 57.
- [3] Argyris, J., and Mlejnek, H.P., 1986, *Die Methode der Finiten Elemente*, Band I, Friedr. Vieweg & Sohn Verlagsgesellschaft mbH, Braunschweig, p. 846.
- [4] Specht, B., 1988, "Modified Shape Functions for the Three-Node Plate Bending Element Passing the Patch Test", *International Journal for Numerical Methods in Engineering*, **26**, pp. 705–715.
- [5] Belloli, A., Niederberger, D., Krnmann, X., Ermanni, P., Morari, M., and Pietrzko, S., 2004, "Vibration control via shunted embedded piezoelectric fibers", *SPIE Smart Structures and Materials - Damping and Isolation*, **5386**, San Diego (CA), March.
- [6] Wierach, P., Monner, H.P., Schönecker, A., and Dürr, J.K., 2002, "Application specific design of adaptive structures with piezoceramic patch actuators", *SPIE Smart Structures and Materials - Industrial and Commercial Applications of Smart Structures Technologies*, **4698**, San Diego (CA), March, pp. 333–341.
- [7] Hagood, N.W., and von Flotow, A., 1991, "Damping of structural vibrations with piezoelectric materials and passive electrical networks", *Journal of Sound and Vibration*, **146**(2), April, pp. 243–268, April 1991.
- [8] Hollkamp, J.J., 1994, "Multimodal passive vibration suppression with piezoelectric materials and resonant shunts", *Journal of Intelligent Material Systems and Structures*, **5**, January, pp. 49–57.
- [9] Wu, S.Y., Turner, T.L., and Rizzi, S.A., 1999, "Piezoelectric shunt vibration damping of f-15 panel under high acoustic excitation", *SPIE Smart Structures and Materials - Passive Damping and Isolation*, **3989**, Newport Beach (CA), March.
- [10] Behrens, S., Moheimani, S.O.R., and Fleming, A.J., 2003, "Multiple mode current flowing passive piezoelectric shunt damper", *Journal of Sound and Vibration*, **266**(5), October, pp. 929–942.
- [11] Crandall, S.H., Karnopp, D.C., Kurtz, E.F., and Pridmore-Brown, D.C., 1968, *Dynamics of Mechanical and Electromechanical Systems*, McGraw-Hill, p. 465.
- [12] Crawley, E.F., and de Luis, J., 1987, "Use of piezoelectric actuators as elements of intelligent structures", *AIAA Journal*, **25**(10), October, pp. 1373–1385.
- [13] Preumont, A., 1991, *Vibration Control of Active Structures - An Introduction*, Kluwer Academic Publishers, Dordrecht, The Netherlands.
- [14] Fuller, C.R., Elliott, S.J., and Nelson, P.A., 1996, *Active Control of Vibration*, Academic Press Limited, Oval Road, London, pp. 24–28.